



Project 47 Clean-Sheet Supersonic Aircraft Engine Design and Performance

Massachusetts Institute of Technology

Project Lead Investigator

Prof. Steven R. H. Barrett
Professor of Aeronautics and Astronautics
Department of Aeronautics and Astronautics
Massachusetts Institute of Technology
77 Massachusetts Avenue – Building 33-322
(617)-452 2550
sbarrett@mit.edu

University Participants

Massachusetts Institute of Technology

- PI: Prof. Steven R. H. Barrett
- FAA Award Number: 13-C-AJFE-MIT, Amendment Nos. 052, 059, and 074
- Period of Performance: March 29, 2019 to August 10, 2021 (with the exception of funding and cost share information, this report covers the period from October 1, 2019 to September 30, 2020)
- Tasks:
 1. Identify mission profiles and operating requirements for propulsion systems.
 2. Develop an engine cycle model for a supersonic aircraft propulsion system.
 3. Assess environmental footprint of an engine for a supersonic transport aircraft.
 4. Assess the effect of variable noise reduction systems on landing and takeoff (LTO) emissions of supersonic aircraft.

Project Funding Level

FAA provided \$1,050,000 in funding and \$1,050,000 in matching funds were provided by the following sources: approximately \$239,000 from the Massachusetts Institute of Technology (MIT) and third-party in-kind contributions of \$177,000 from Byogy Renewables, Inc., and \$634,000 from NuFuels LLC.

Investigation Team

- Prof. Steven Barrett (MIT) serves as PI for ASCENT Project 47 as head for the Laboratory for Aviation and the Environment. Prof. Barrett coordinates internal research efforts and maintains communication between investigators in the various MIT research teams.
- Dr. Raymond Speth (MIT) serves as co-investigator for Project 47. Dr. Speth directly advises student research in the Laboratory for Aviation and the Environment focused on assessment of fuel and propulsion system technologies targeting reduction of aviation's environmental impacts. Dr. Speth also coordinates communication with FAA counterparts.
- Dr. Jayant Sabnis (MIT) serves as co-investigator for Project 47. Dr. Sabnis co-advises student research in the Laboratory for Aviation and the Environment. His research interests include turbomachinery, propulsion systems, gas turbine engines, and propulsion system-airframe integration.
- Dr. Choon Tan (MIT) serves as co-investigator for Project 47. Dr. Tan directly advises student research in the Gas Turbine Laboratory focused on unsteady and three-dimensional flow in turbomachinery and propulsive devices, aerodynamic instabilities in aircraft gas turbine engines, and propulsion systems.
- Mr. Prashanth Prakash is a PhD student in the Laboratory for Aviation and the Environment. Mr. Prakash is responsible for developing engine models in the Numerical Propulsion System Simulation (NPSS) tool, for developing the combustor reactor network model, and for analyzing the sensitivity of engine emissions to design parameters.



- Mr. Laurens Voet is a PhD student in the Gas Turbine Laboratory. Mr. Voet is responsible for determining propulsion system requirements for supersonic aircraft designs, for relating the noise footprint to the relevant engine parameters, for estimating the effective perceived noise level (EPNL) for given aircraft trajectories, and for proposing clean-sheet engine design solutions to reduce its noise footprint.

Project Overview

A number of new civil supersonic aircraft designs are currently being pursued by industry in different Mach regimes and for different size classes (e.g., supersonic business jets at low-supersonic Mach numbers and airliners at high-supersonic Mach numbers). Compared with those for subsonic aircraft, engines for supersonic aircraft present unique challenges in terms of their fuel consumption, noise, and emissions impacts because of their unique operating conditions. The propulsion systems currently proposed by the industry are developed around the core (high-pressure compressor, combustor, and high-pressure turbine) of existing subsonic engines, with modifications to the low-pressure spool (fan and low-pressure turbine).

ASCENT Project 47 aims to evaluate the design space of clean-sheet engines designed specifically for use on civil supersonic aircraft, and to determine the resulting environmental performance of such engines. Unlike previous commercial supersonic engines, which were adapted from military aircraft, or planned propulsion systems derived from current commercial engines, a clean-sheet engine takes advantage of recent advances in propulsion system technology to significantly improve performance and reduce emissions and noise footprints. This project will quantify these benefits for a range of engine designs relevant to currently proposed civil supersonic aircraft.

Specific goals of this research include:

- Development of a framework for quantifying the noise and emissions footprints of propulsion systems used on civil supersonic aircraft.
- Assessment of the difference in environmental footprint between a derived engine and a clean-sheet engine for a civil supersonic aircraft.
- Assessment of variable noise reduction systems used during noise certification of Supersonic Level 1 (SSL1) type aircraft and their effect on landing and take-off (LTO) emissions.
- Development of a roadmap for technology development, focusing on reducing the environmental footprint associated with engines for civil supersonic aircraft.

A summary of accomplishments to date include the following:

- A survey of supersonic transport concepts and existing designs was carried out, and the Stanford University Aerospace Vehicle Environment (SUAVE) was selected to analyze mission profiles and derive propulsion system requirements.
- Multiple engine models were developed in the NPSS tool. The baseline engine chosen for the derivative engine analysis was the CFM56-5B engine.
- The engine cycle model was used to evaluate the sensitivities of performance measures to design variables, technology assumptions, and propulsion system requirements.
- A reactor network framework was developed to estimate NO_x emissions. The model was calibrated to the International Civil Aviation Organization (ICAO) data for the CFM56-5B3 engine.
- A framework was set up to estimate the noise footprint sound pressure level (SPL), tone-corrected perceived noise level (PNLT) and effective perceived noise level (EPNL) of the engine given the relevant engine parameters using a semi-empirical model.
- Preliminary estimates have been made of the difference of pollutant emissions of engines for supersonic transport aircraft flying trajectories with and without variable noise reduction systems (VNRS).

Task 1 – Identify Mission Profiles and Operating Requirements for Propulsion Systems

Massachusetts Institute of Technology

Objectives

The first objective of this task is to identify representative mission profiles of commercial supersonic transport aircraft (i.e., characterize stages of the mission by defining parameters such as climb rates and accelerations). A second objective is to

use these mission profiles and representative aircraft parameters (e.g., wing area, drag and lift polars) of civil supersonic aircraft operating in different Mach regimes to derive propulsion system requirements for supersonic aircraft.

Research Approach

The mission profile of the NASA Supersonic Technology Concept Aeroplane (STCA) is used to get propulsion system requirements (Berton, 2019). The four critical sizing points of the NASA STCA, as illustrated in Table 1, are used in a multiple-design-point (MDP) model in the engine design process.

Table 1. Propulsion system requirements (per engine) for STCA. The top-of-climb conditions are chosen as the aerodynamic design point for any component that is purpose-designed for the application.

	Sea level static (SLS)	Takeoff (TO)	Top-of-climb (TOC)	End-of-cruise (EOC)
Altitude [kft]	0	0	41	51
Mach [-]	0	0.25	1.4	1.4
Thrust [lbf]	16,617	14,140	5,500	3,300

Mission requirements for other aircraft designs will be obtained through collaborations with ASCENT Project 10.

Publications

N/A

Outreach Efforts

None

Awards

None

Student Involvement

N/A

Plans for Next Period

Define the propulsion system requirements for different missions of supersonic transport aircraft (expected completion: April 2021)

References

Berton, J. & Geiselhart, K. (2019). NASA 55-tonne Supersonic Transport Concept Aeroplane (STCA) release package. NASA GRC/NASA LaRC.

Task 2 – Develop an Engine Cycle Model for a Supersonic Aircraft Propulsion System

Massachusetts Institute of Technology

Objectives

The objectives of this Task were to: 1) develop an engine cycle deck to analyze derivative and clean-sheet propulsion systems for commercial supersonic aircraft, 2) assess the sensitivities of engine performance metrics to constraints and propulsion system requirements to analyze the impact of design requirements and technology constraints on the engine performance, and 3) evaluate the design space constraints imposed by a constraint donor engine core on the environmental footprint.

Research Approach

The NPSS software (Claus, 1991) was chosen to develop the engine cycle decks for clean-sheet and derivative engines because it is an industry standard tool, which facilitates future collaboration with other users of the tool.



Donor engine model

To develop the derivative engine, a baseline engine is first chosen and modeled. The CFM56-5B engine was chosen for this Task because it was the initial donor engine for the proposed GE Affinity engine. The engine architecture of the donor engine is illustrated in the bottom half of Figure 1. The baseline engine was modeled using published data from Jane's Aero Engines and data published in the Emissions Databank (EDB) by the European Union Aviation Safety Agency (EASA). The thrust versus fuel flow characteristic of the engine model is compared with data from the EDB of six CFM56 variants. The root mean square (RMS) error between the engine model results and the EDB data is 1.3%.

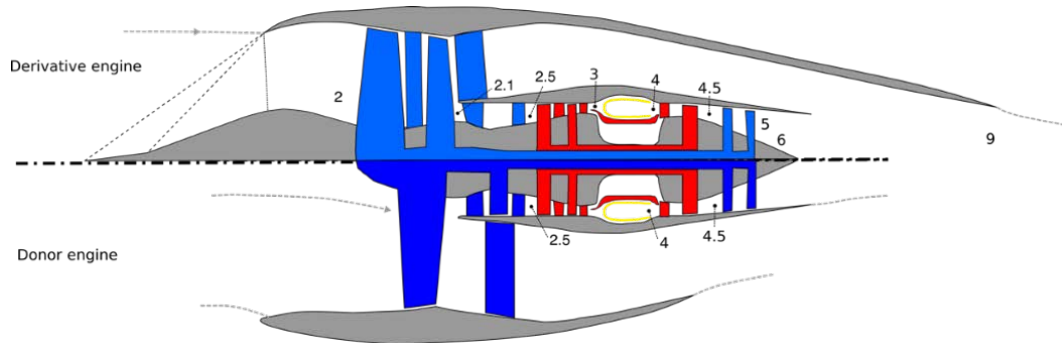


Figure 1. Engine architecture schematic. Lower half shows the subsonic donor engine. The high spool (red) core is used in the derivative engine along with modifications to the inlet, fan, and nozzle as shown on the top half.

Derivative engine model

The thrust requirements of the derivative engine are given in Table 1. As shown in the engine architecture diagram in Figure 1, the derivative engine for supersonic application uses the high-pressure core of the donor subsonic engine. The low-pressure spool consists of a two-stage fan and a low-pressure turbine (LPT). An external compression supersonic inlet with two oblique shock stages is mounted upstream of the fan, with a pressure recovery modeled using standard oblique shock equations. A fully mixed, variable area nozzle is added downstream of the LPT. The engine is designed such that the nozzle is at the cusp of choke at takeoff conditions to avoid shock-cell noise. Polytropic efficiencies of the turbomachinery components are set to values representative of the CFM56-5B3 technology level. The map scalars of the turbomachinery components in the engine cycle model, the flow areas, and the cooling bleed flow fractions of the CFM56 donor engine core are applied as fixed constants to the derivative engine model.

Clean-sheet engine model

The clean-sheet engine is also designed to meet the propulsion system requirements outlined in Table 1. The engine architecture for the clean-sheet design is the same as the derivative design. However, all the components for the clean-sheet engine, along with the high-pressure core, are purpose-designed. To have a fair comparison between the derivative and clean-sheet engine, the polytropic efficiencies of the turbomachinery are set to the CFM56 values to model the same technology level.

Engine performance sensitivities

Sensitivities of engine performance metrics to constraints and propulsion system requirements are calculated for both the clean-sheet and derivative engine to analyze the impact of design requirements and technology constraints on the engine performance. A design vector, x , containing propulsion system requirements (net thrust, F_n , turbine inlet temperature, T_{t4} , flight parameter, θ_{01}) and design variables (mixer pressure ratio, Mix_{PR} , fan pressure ratio, π_{fan} , HPC pressure ratio, π_{hpc}), and an objective vector, u , containing environmental response and performance metrics (specific fuel consumption, SFC, NO_x emission index, $EINO_x$, bypass ratio, BPR) are defined as:



$$\vec{x} = \begin{bmatrix} F_n \\ T_{I4} \\ \theta_0 \\ \text{Mix}_{PR} \\ \pi_{FPR} \\ \pi_{HPC} \end{bmatrix} \quad \begin{array}{c} \text{Requirements/} \\ \text{constraints} \\ \\ \text{Design Variables} \\ \\ \text{Response/ performance} \\ \text{metrics} \end{array} \quad \vec{u} = \begin{bmatrix} F_n \\ T_{I4} \\ \theta_0 \\ \text{Mix}_{PR} \\ \pi_{FPR} \\ \pi_{HPC} \\ \text{SFC} \\ \text{EINO}_x \\ \text{BPR} \\ \vdots \end{bmatrix} \quad (1)$$

The sensitivities of the objective vector with respect to the design vector

$$\frac{dU}{dx} = \begin{bmatrix} I_{n \times n} \\ \frac{\partial(SFC)}{\partial(F_n)} & \frac{\partial(SFC)}{\partial(T_{I4})} & \frac{\partial(SFC)}{\partial(\theta_0)} & \frac{\partial(SFC)}{\partial(FPR)} & \dots \\ \frac{\partial(EINO_x)}{\partial(F_n)} & \frac{\partial(EINO_x)}{\partial(T_{I4})} & \frac{\partial(EINO_x)}{\partial(\theta_0)} & \frac{\partial(EINO_x)}{\partial(FPR)} & \dots \\ \vdots & \vdots & \vdots & \vdots & \vdots \end{bmatrix} \quad (2)$$

are calculated using a 5-point finite difference stencil applied across the engine cycle model. The sensitivities of the engine model are also used in conjunction with the noise and emission model to assess sensitivities of the environmental footprint with respect to engine design parameters.

Derivative engine design space constraints

A first-principle approach is used to evaluate design space constraints imposed by the donor core on the environmental footprint of the derivative engine. The engine cycle deck described above is used to calculate the engine performance in terms of SFC, emissions index, and noise of both the derivative and clean-sheet engine. Engine gaseous NO_x emissions are quantified using the P₃-T₃ method (DuBois and Paynter, 2006). The emissions index of NO_x is assumed to be proportional to P_{t3}^{0.4} and a polynomial fit in T_{t3}, constructed based on engine emission data from the ICAO emission data bank, leading to the correlation

$$\frac{EI(NO_x)}{P_{t3}^{0.4}} = 6.26 \cdot 10^{-8} T_{t3}^3 - 0.00117 T_{t3}^2 + 0.0074 T_{t3} - 15.04 \quad (3)$$

The engine jet mixing noise is quantified using the SAE ARP876 jet noise power level method. The jet noise power, Π_{jet}, is non-dimensionalized using the ambient density, ρ₀, the ambient speed of sound, c₀, and the jet area, A_{jet}. The density exponent, ω, accounts for the effect of density on noise in heated jets. The power deviation factor, P, accounts for the variation of the classical 8-th power law by Lighthill.

$$\Pi_{jet}^* = \frac{\Pi_{jet}}{\rho_0 c_0^3 A_{jet}} = (6.67 \cdot 10^{-5}) \cdot P \cdot \left(\frac{\rho_{jet}}{\rho_0}\right)^\omega \cdot \left(\frac{V_{jet}}{c_0}\right)^8 \quad (4)$$

$$PWL_{jet} = 10 \log_{10} \Pi_{jet}^* - \frac{\Pi_{ref}}{\rho_0 c_0^3 A_{jet}} \quad (5)$$

Milestones

Multiple engine models were developed in NPSS. The donor engine for the supersonic derivative core is chosen to be the CFM56-5B engine. The derivative engine model was used to evaluate the impact of design space constraints on the performance of the engine relative to the clean-sheet model.

Major Accomplishments

Engine performance sensitivities

Sensitivities of engine performance metrics with respect to design parameters are illustrated in Figure 2 for both the clean-sheet and derivative engine. In both cases we find that increasing the fan-pressure ratio (FPR) results in an increase in SFC. This is due to the increase in jet velocity and the corresponding reduction in the propulsive efficiency. Similarly, increasing the FPR also results in an increase in the compressor exit temperature and therefore results in an increase in the emissions index of NO_x . Increasing the turbine inlet temperature (T_{t4}) results in an improvement in the thermal efficiency. However, it only results in a decrease in thrust-specific fuel consumption (TSFC) for the clean-sheet engine. This is due to the operation of the derivative core being a function of the turbine inlet temperature.

The derivative engine's high-pressure compressor (HPC) pressure ratio decreases as turbine inlet temperature are increased. This reduction in HPC pressure ratio as T_{t4} is increased results in a net increase in TSFC unlike the clean-sheet engine. Similarly, the HPC pressure ratio decreases as the FPR of the derivative engine is increased. The sensitivity of the TSFC of the derivative engine to the FPR is approximately twice as much as the clean-sheet engine due to the decreased thermal efficiency from the lower HPC pressure ratio and the decrease in propulsive efficiency from the increased FPR.

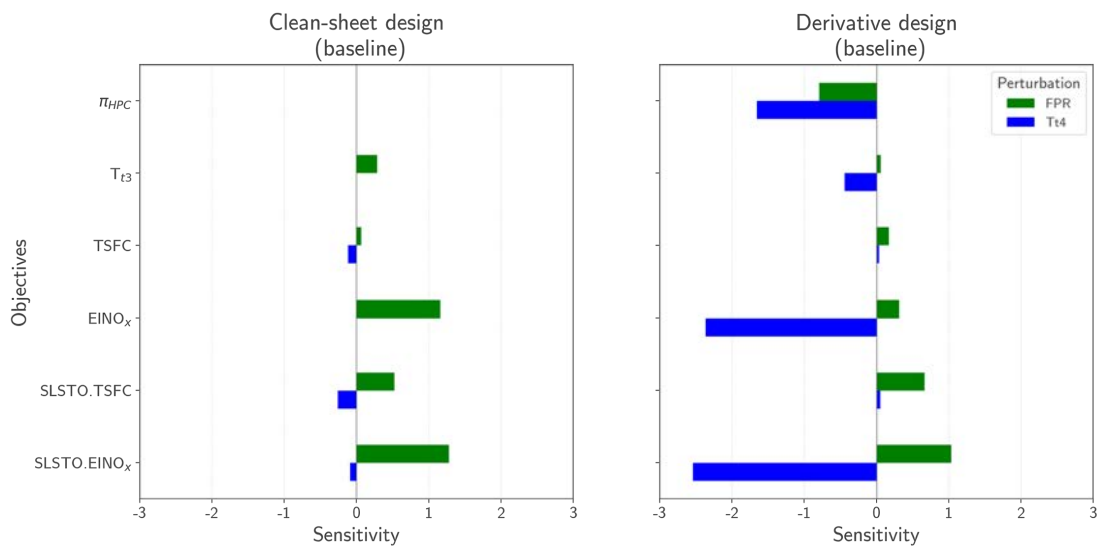


Figure 2. Sensitivities of engine performance parameters (HPC pressure ratio, π_{hpc} , compressor discharge temperature, T_{t3} , specific fuel consumption, $TSFC$, and NO_x emission index, $EINO_x$, at both design and sea-level static takeoff conditions) to engine design parameters (fan pressure ratio, FPR, and turbine inlet temperature, T_{t4}) for the clean-sheet (left) and derivative (right) engine.

Derivative engine design space constraints

Because the core of the derivative engine is sized by the donor-engine (CFM56) cycle, the pressure ratio of the high-pressure compressor of the derivative engine is not an independent design variable (in contrast to a clean-sheet engine where the HPC pressure ratio is a design variable that can be optimized). The design space of the derivative engine is illustrated in Figure 3. The core of the derivative engine also has cooling flows for the high-pressure turbine sized by the donor engine cycle. Therefore, there are regions of the design space where insufficient cooling flow can result in turbine metal blade temperatures exceeding the set limits. Therefore, the constraints from the donor core limit the feasible design space that can be used for the derivative engine.

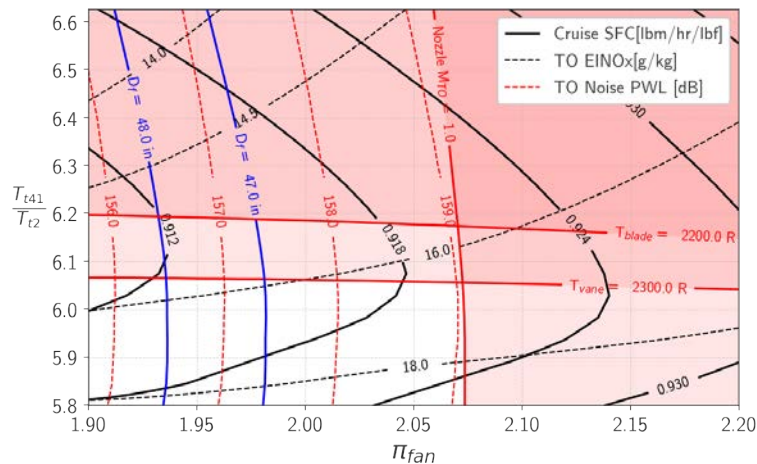


Figure 3. Design space of the derivative engine: turbine inlet temperature over compressor inlet temperature ratio, T_{t41}/T_{t2} , vs. fan pressure ratio, π_{fan} , at the engine aerodynamic design point. The performance contours are plotted at different engine operating points; cruise for specific fuel consumption (SFC) and takeoff for noise power level, PWL, and NOx emission index, $EINO_x$. Unshaded region represents the feasible design space of the derivative engine. The resulting fan diameter, D_f , for different designs in the design space is indicated.

Publications

None

Outreach Efforts

Mr. Prashanth Prakash and Mr. Laurens Voet gave a presentation titled "Clean-sheet supersonic engine design and performance" at the virtual ASCENT meeting on September 30, 2020.

Awards

None

Student Involvement

This task was conducted primarily by Prashanth Prakash, a graduate research assistant working under the supervision of Dr. Jayant Sabnis, Dr. Raymond Speth, and Dr. Choon Tan.

Plans for Next Period

Various degrees of derivative engine models are to be developed, ranging from an "off-the-shelf" repurposing of an entire engine to using only the core of an existing engine (expected completion: May 2021).

A clean-sheet approach that ranges from redesigning a core with existing technology (e.g., metallurgy, cooling technology) to using new technology (e.g., advanced materials) and adaptive cycles to meet contrasting requirements at supersonic cruise and sea-level takeoff (expected completion: December 2021).

References

Claus, Russell W., et al. "Numerical propulsion system simulation." *Computing Systems in Engineering* 2.4 (1991): 357-364.
 D. DuBois and G. C. Paynter, "Fuel Flow Method 2 for estimating aircraft emissions," SAE Technical Paper, 2006.



Task 3 – Assess Environmental Footprint of an Engine for a Supersonic Transport Aircraft

Massachusetts Institute of Technology

Objective

The objective of this Task is to develop models to assess the environmental footprint of a supersonic transport aircraft. Models for both the noise footprint and the emissions footprint will be developed.

Research Approach

The flow chart in Figure 4 illustrates the approach to model the environmental footprint of engines for supersonic transport.

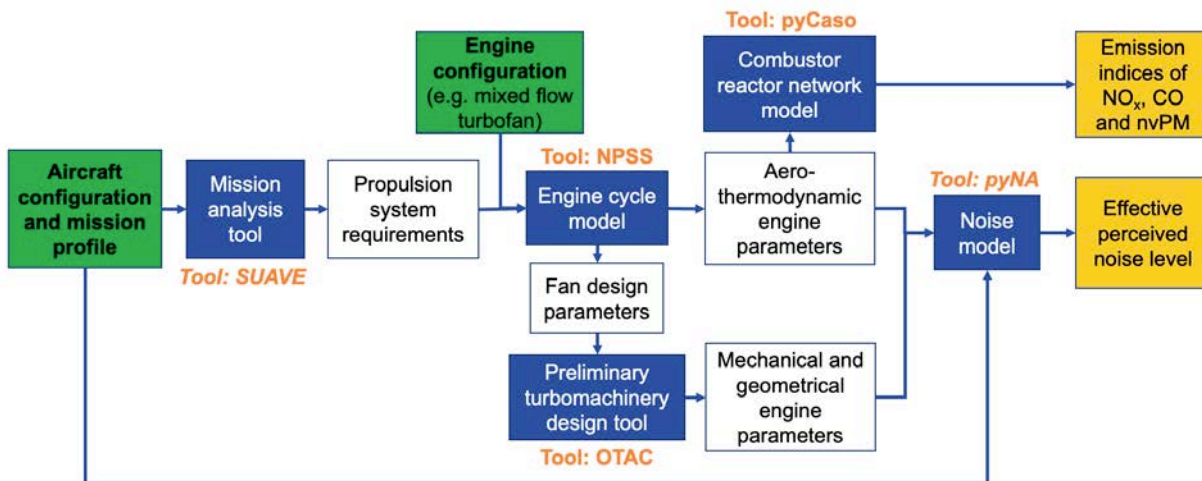


Figure 4. Overview of the framework to model environmental footprint of engines for supersonic transport (SST). The mission analysis is performed using the Stanford University Aerospace Vehicle Environment (SUAVE), the engine cycle model is made in the Numerical Propulsion System Simulation (NPSS) tool, the combustor reactor network model (pyCaso), and the noise model (pyNA) are used to calculate emission indices and effective perceived noise levels of the engines.

Emissions modeling

A chemical reactor network combustor model (pyCaso) was developed to assess the emissions of the engines for supersonic transport. The combustor model represents CFM56-TechInsertion rich-quench-lean (RQL) combustor technology. The combustor model is illustrated in Figure 5. A series of perfectly stirred reactors in parallel, representing the primary zone of the combustor, are coupled to a secondary zone plug flow reactor. Similar to the engine model, the emission characteristics of the combustor model are validated against publicly available data from the EDB.

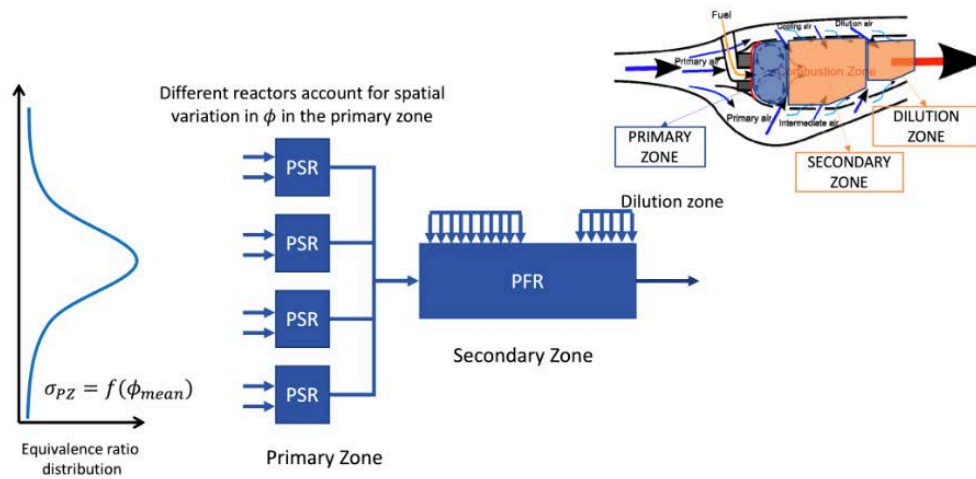


Figure 5. Chemical reactor network combustor model: a series of perfectly stirred reactors (PSR) in parallel, representing the primary zone, combined in parallel with a secondary zone plug flow reactor (PFR). The series of perfectly PRF represents a gaussian distribution, with standard deviation, σ_{PZ} being a function of the mean equivalence ratio, ϕ_{mean} .

Noise footprint modeling

A python Noise Assessment (*pyNA*) model was developed to estimate the engine noise footprint as well as assess the sensitivities of the noise footprint with respect to relevant engine variables. The steps involved in estimating the effective perceived noise level (EPNL), given engine cycle and fan parameters, are shown in Figure 6.

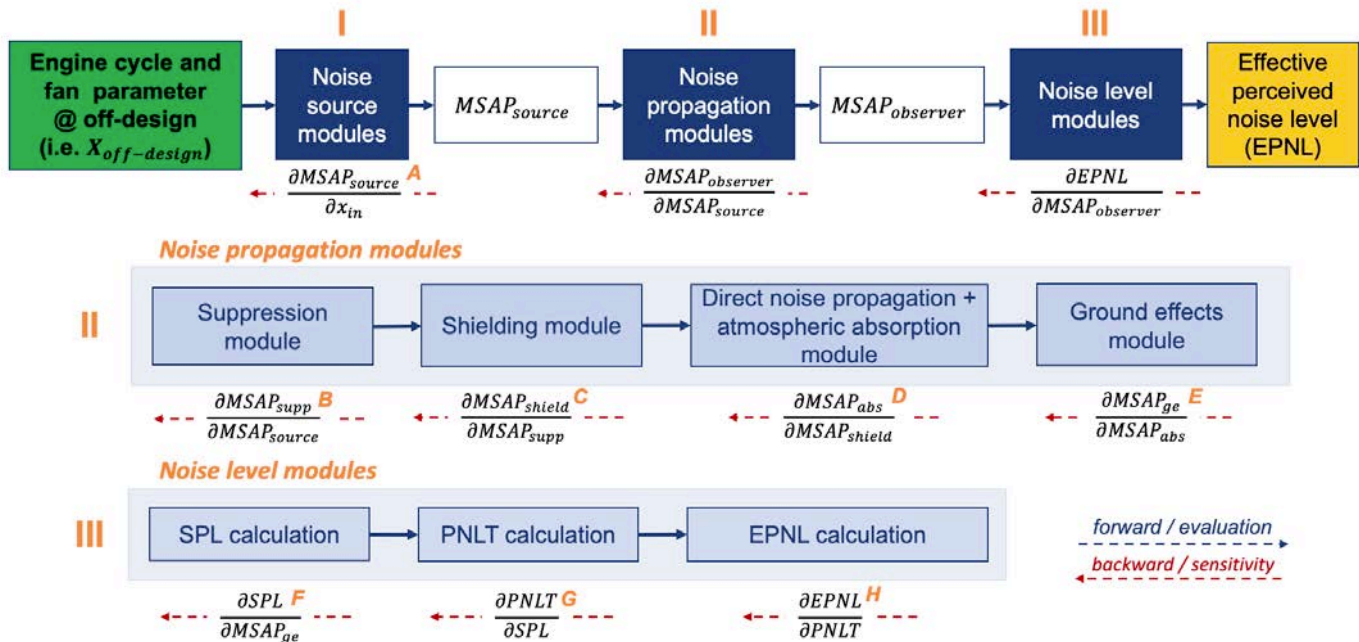


Figure 6. Flow chart of the python Noise Assessment (*pyNA*) model showing the different modules required to estimate the EPNL from engine cycle and fan parameters.

The different noise modules in *pyNA*, as shown in Figure 6, are developed using the methods from literature listed in Table 2, based on the Aircraft Noise Prediction Program (ANOPP) theoretical manual (Zorunski, 1981).



Table 2. Methods for the noise source, propagation, and levels modules.

Module	Method from literature
Noise source modules <ul style="list-style-type: none"> • Jet mixing noise • Jet shock-cell noise • Combustor noise • Fan broadband and tones (inlet and discharge) • Airframe noise 	Single-stream, shock-free jet mixing noise (SAE ARP876, 2012) Circular jet shock cell noise (SAE ARP876, 2012) Emmerling method FAA-RD-74-125 (Emmerling et al., 1976) Heidmann method NASA TM X-71763 (Heidmann, 1975) <ul style="list-style-type: none"> • with GEAE revision NASA CR-195480 for BB (Kontos et al., 1996) • with AlliedSignal revision for RS tones (Hough et al., 1996) • with fan treatment NASA CR-202309 (Kontos et al., 1996) Fink method FAA RD-77-29 (Fink, 1977) with HSR calibration NASA CR-2004-213014 (Golub et al., 2004)
Noise propagation modules <ul style="list-style-type: none"> • Spherical spreading/ characteristic impedance • Atmospheric absorption • Ground reflection and attenuation • Wing shielding module 	R^2 law and characteristic impedance ratio Exponential decay from source based on absorption coefficient Chien-Soroka method (Chien et al., 1975) Maekawa method (copied shielding factors from STCA) (Maekawa, 1968)
Certification Noise Levels modules <ul style="list-style-type: none"> • Perceived noise level, tone corrected (PNLT) • Effective perceived noise level (EPNL) 	ICAO Annex 16 Volume I: Aircraft noise App. 2-13 (ICAO, 2008) ICAO Annex 16 Volume I: Aircraft noise App. 2-13 (ICAO, 2008)

The *pyNA* noise model is developed to have two different operating modes:

- **A forward, evaluation mode:** using engine off-design variables at takeoff/approach to calculate the certification EPNL (blue arrows in Figure 6). The noise source modules as well as the noise during the takeoff trajectory are verified with the NASA STCA noise assessment (Berton, 2019). The takeoff trajectory of the NASA STCA, including the noise source verification point are shown in Figure 7.
- **A backward, sensitivity mode:** calculating derivatives of the noise footprint with respect to engine off-design variables at takeoff/approach (red arrows in Figure 6). The partial derivatives of each module in Figure 6 are calculated using a pyTorch autograd implementation. The pyTorch derivative implementation is verified using a finite-difference scheme or analytical derivatives.

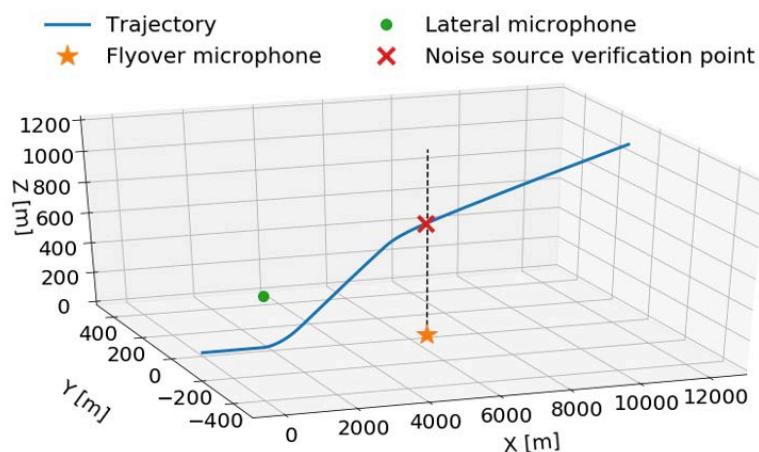


Figure 7. Standard takeoff trajectory of the 55-tonne STCA including lateral and flyover microphone positions. The noise source verification point is indicated with a red X.

Milestones

A chemical reactor network-based combustor model was developed, and NO_x and CO emissions were calibrated to the EDB data using combustor inlet values obtained from the NPSS model of the CFM56-5B engine.

A model estimating the static noise database from relevant engine parameters, the static-to-flight noise projection, and the certification noise levels was set up.

Major Accomplishments

Emissions model

A framework was developed to estimate the NO_x and CO emissions indices of the donor engine, given the relevant engine parameters using a reactor network model. A comparison of the model developed and the EDB data is shown in Figure 8. The derivative and clean-sheet engine analyzed in the work described here assumes that the combustor technology used is similar to that of the donor engine and therefore the calibrated parameters are assumed to hold for the clean-sheet engine as well. A soot model to estimate the non-volatile particulate matter (nvPM) concentrations is currently being integrated into the combustor model.

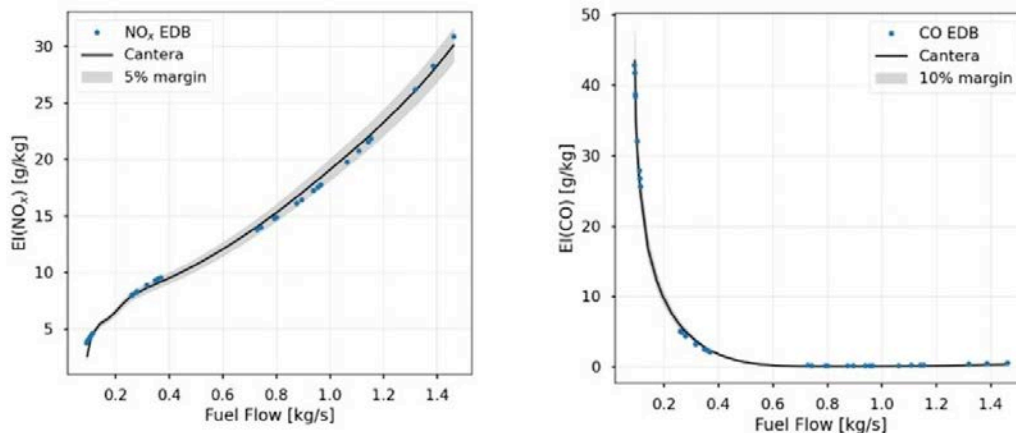


Figure 8. Comparison of NO_x emission indices (left) and CO emission indices (right) of the combustor model and ICAO data from the EDB.

Noise model (pyNA)

A framework was set up to estimate the noise footprint (SPL, PNLT, and EPNL) of the engine given the relevant engine parameters using a semi-empirical model. As an example, the jet mixing noise source SPL and the overall sound pressure level (OASPL) distribution are shown in Figure 9. The tone-corrected perceived noise level (PNLT) for jet mixing noise source, measured at the flyover microphone, is shown in Figure 10.

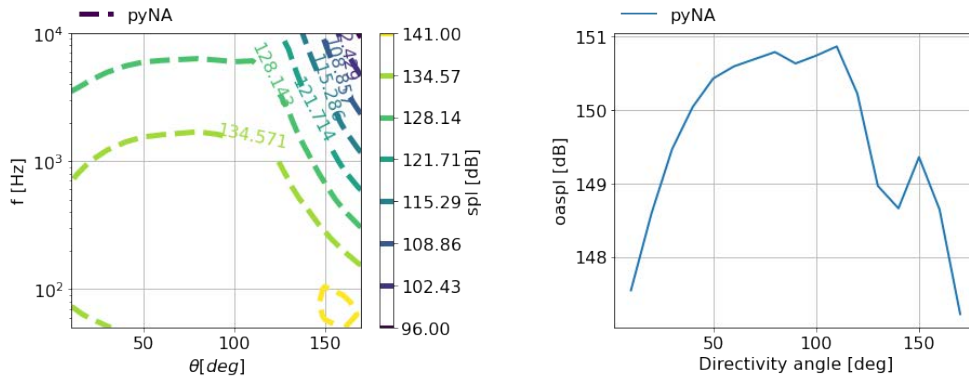


Figure 9. Jet mixing source SPL spectral and directivity distribution (left) and overall sound pressure level (OASPL) directivity distribution (right) at the noise source verification point.

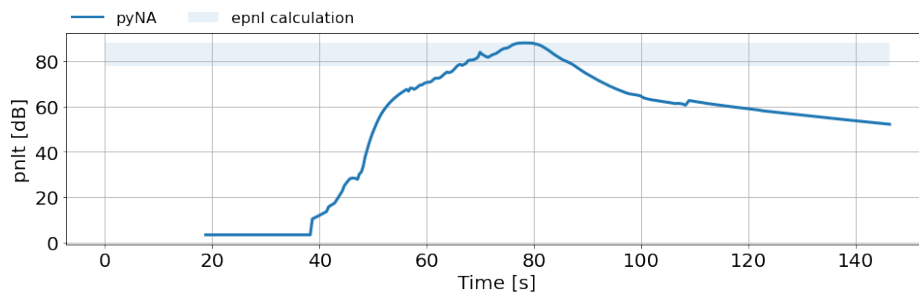


Figure 10. Jet mixing tone-corrected PNLt at the flyover microphone for the NASA STCA Standard take-off trajectory.

Table 3 shows the effective perceived noise level of the pyNA noise assessment for the NASA STCA aircraft for the lateral, flyover, and approach microphones. The EPNL are verified with the NASA STCA noise assessment. The individual EPNL have a maximum error $\Delta EPNL_{max} < 5\%$; the total noise levels have an error $\Delta EPNL < 0.5\%$ (Berton, 2019).

Table 3. pyNA results for the effective perceived noise levels for the lateral, flyover and approach microphone for the Standard take-off trajectory of the NASA STCA.

	Lateral [EPNdB]	Flyover [EPNdB]	Approach [EPNdB]
Fan inlet *	50.2	35.5	72.3
Fan exit *	77.1	71.7	91.0
Combustor	77.2	73.5	79.9
Jet mixing	94.8	88.0	90.5
Total	95.2	88.7	95.9

The pyNA backward sensitivity mode is used to calculate sensitivities of EPNL with respect to off-design parameters. The sensitivity results can be seen in Figure 11. The x-axis of the sensitivity plots is limited to the region in which PNLt contributes to the EPNL calculation (i.e., region 10dB below $PNLT_{max}$).

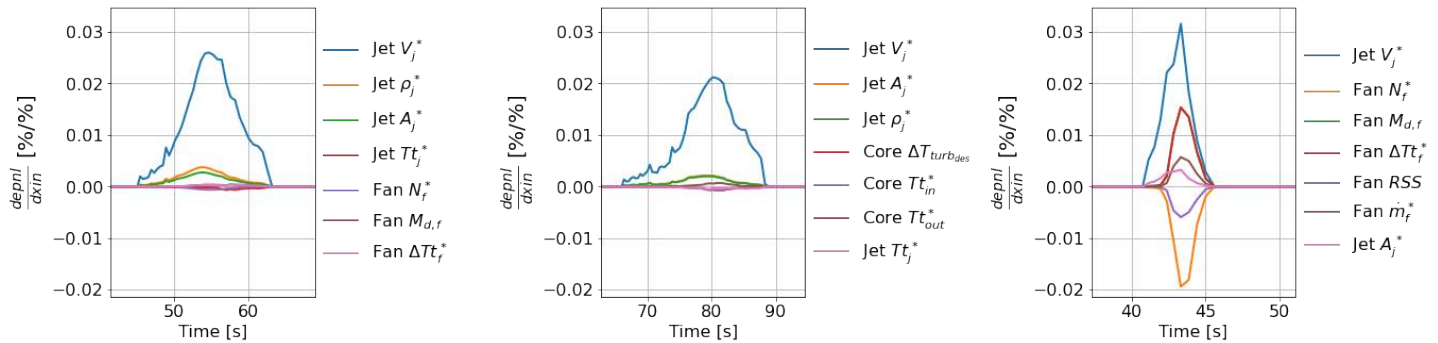


Figure 11. Sensitivities of the EPNL at the lateral, flyover and approach microphone with respect to engine off-design variables (x_{in}).

Publications

None

Outreach Efforts

Mr. Prashanth Prakash and Mr. Laurens Voet gave a presentation titled "Clean-sheet supersonic engine design and performance" at the virtual ASCENT meeting on September 30, 2020.

Awards

None

Student Involvement

This Task was conducted primarily by Prashanth Prakash and Laurens Voet, graduate research assistants working under the supervision of Dr. Jayant Sabnis, Dr. Raymond Speth, and Dr. Choon Tan.

Plans for Next Period

- Extend the combustor model to include representation of staged combustors, and incorporate soot modeling capabilities to enable estimation of nvPM emissions (expected completion: May 2021)
- Enhance the noise model to calculate sensitivities between relevant engine parameters and the resulting noise footprint (expected completion: March 2021)
- Begin development of a preliminary turbomachinery design tool to determine noise-relevant geometrical engine parameters for an engine configuration (expected completion: August 2021)

References

- W. E. Zorumski, Aircraft Noise Prediction Program Theoretical Manual Part 1-2, Technical report, NASA, 1982.
- Society of Automotive Engineers, ARP-876: Gas Turbine Jet Exhaust Noise Prediction, SAE, 1994.
- J. Emmerling, S. Kazin, R. Matta, Core engine noise program. Volume III. Prediction methods – Supplement I: Extension of prediction methods, Technical report, General Electric Co Cincinnati OH Aircraft Engine Business Group, 1976.
- M. F. Heidmann, Interim prediction method for fan and compressor source noise (NASA-TM-x71763), 1995.
- K. B. Kontos, B. Janardan, P. Gliebe, Improved NASA-ANOPP noise prediction computer code for advanced subsonic propulsion systems. Volume 1: ANOPP evaluation and fan noise model improvement (NASA CR-195480), 1996.
- K. B. Kontos, R. E. Kraft, P. R. Gliebe, Improved NASA-ANOPP noise prediction computer code for advanced subsonic propulsion systems. Volume 2: Fan suppression model development (NASA-CR-202309), 1996.
- J. W. Hough, D. S. Weir, Aircraft noise prediction program (ANOPP) fan noise prediction for small engines (NASA-CR-198300), 1996.
- M. R. Fink, Airframe noise prediction method, Technical report, United Technologies Research Center East Hartford, CT, 1977.
- Golub, Robert, John W. Rawls Jr, and Jessie C. Yeager. High Speed Research Noise Prediction Code (HSRNOISE) User's and Theoretical Manual, 2004.

C. Chien, W. Soroka, Sound propagation along an impedance plane, *Journal of Sound and Vibration* 43 (1) (1975) 9–20
 Z. Maekawa, Noise reduction by screens, *Applied Acoustics* 1 (3) (1968) 157–173.
 ICAO, Annex 16 environmental protection. Volume I: Aircraft engine emissions (eight edition), 2017.
 Berton, J. & Geiselhart, K. (2019). NASA 55-tonne Supersonic Transport Concept Aeroplane (STCA) release package. NASA GRC/NASA LaRC.

Task 4 – Assess the Effect of Variable Noise Reduction Systems on LTO Emissions for Engines for Supersonic Transport Aircraft

Massachusetts Institute of Technology

Objective

The objective of this Task is to assess the effects of variable noise reduction systems (VNRS) on the takeoff and climb emissions for supersonic transport engines. The objective of this task is to determine whether the current LTO cycle is relevant for supersonic transport engines and if not, characterize what such a relevant LTO cycle would look like.

Research Approach

The approach to address the above-mentioned research objectives is shown in Figure 12. We start from a supersonic level 1-type aircraft (NASA STCA), and an engine model for that aircraft (a CFM56-based derivative). These are input in a takeoff trajectory model that is coupled to a noise model. Minimizing the noise footprint using a variable noise reduction system gives us a programmed lapse rate (PLR), characterized by a power setting schedule as a function of time, $PS(t)$. This power setting schedule is put into a combustor model to estimate takeoff emissions (i.e., Method 1 in Figure 12). These emissions are compared to a baseline trajectory, using a simple power setting schedule, without VNRS being applied (i.e., Method 2 in Figure 12). We are interested in comparing the takeoff emissions of both these methods.

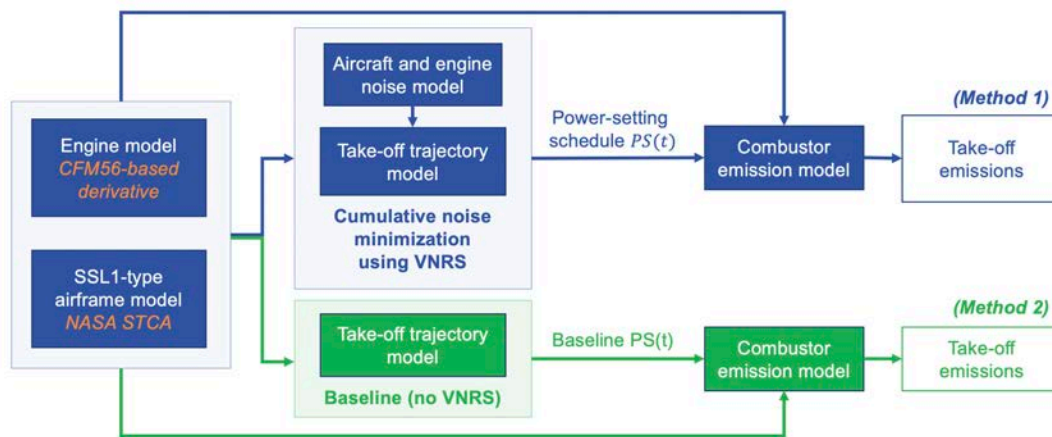


Figure 12. Flow chart of the approach to estimate the effect of VNRS on takeoff emissions of engines for supersonic transport.

Milestone

A first estimate has been made of the difference of pollutant emissions of engines for supersonic transport aircraft flying trajectories with and without VNRS.

Major Accomplishments

The takeoff and climb emissions of the NASA STCA "Standard" (having pilot-initiated cutback only) and "Advanced" (having a programmed lapse rate on top of a pilot-initiated cutback) takeoff trajectory are compared in Figure 13 (Berton, 2019). The instantaneous emission indices for NO_x and CO are calculated using a T_3-P_3 method. It can be seen in these graphs, that applying a PLR affects both NO_x and CO emission indices.

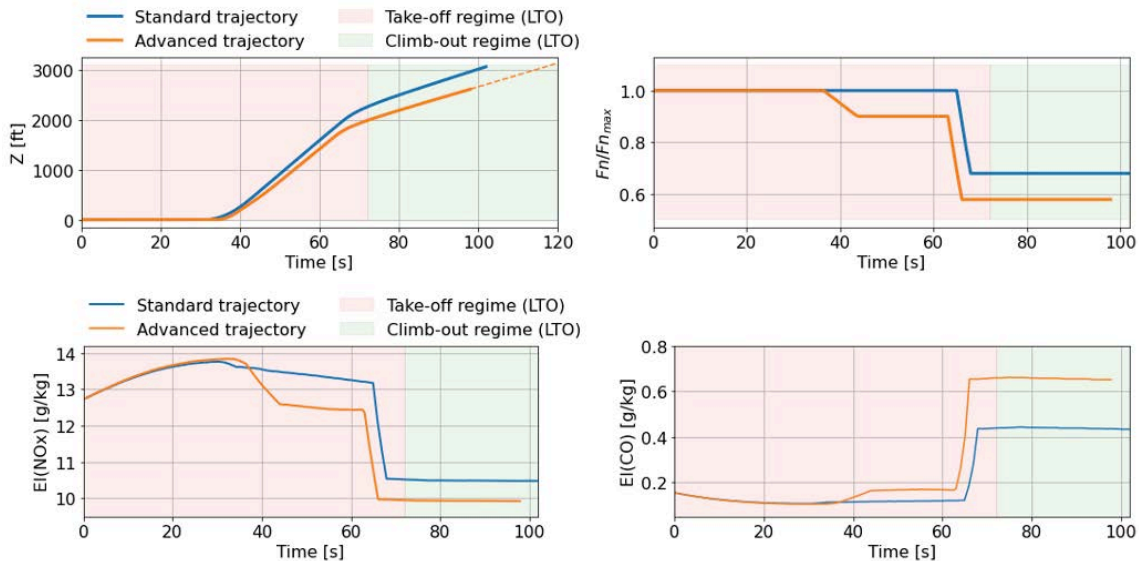


Figure 13. Comparison of NASA STCA Standard and Advanced takeoff trajectory (top left) and power setting (top right). The instantaneous emission indices during flight are compared for both NO_x (bottom left) and CO (bottom right).

To quantify the overall difference in emissions, the total mass of pollutants emitted during the entire takeoff and climb regime of the current LTO cycle are calculated, thereby extrapolating the climb regime to 192 seconds, as shown in Table 4. A difference of 11% for NO_x and 30% for CO is observed between the Standard and Advanced NASA STCA trajectory, mainly caused by applying the variable noise reduction system, the PLR.

Table 4. Comparison of NO_x and CO emissions mass for takeoff and climb-out regime of the conventional LTO cycle for the Standard and Advanced NASA STCA takeoff trajectory.

Regime	Std. trajectory m_{NO_x} [g]	Adv. trajectory m_{NO_x} [g]	Std. trajectory m_{CO} [g]	Adv. trajectory m_{CO} [g]
Take-off	877	817	9	11
Climb-out	767	638	32	42
Total	1644	1455	41	53
$\Delta_{std-adv.}$	-11.5 %		+29.3 %	

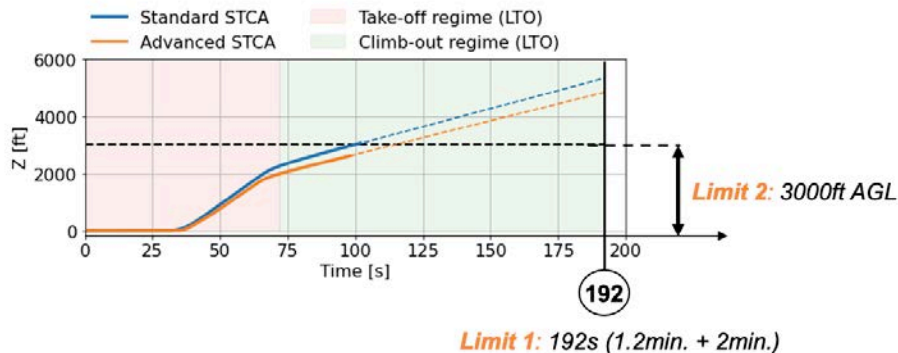


Figure 14. Comparison of NASA STCA Standard and Advanced takeoff trajectory (top left) and power setting schedule (top right). The instantaneous emission indices during flight are compared for both NO_x (bottom left) and CO (bottom right).



The objective of the current emission standards is to limit pollutant emissions below 3000 ft above ground level (AGL). Looking at both the NASA Standard and Advanced takeoff trajectory, it can be seen that applying PLR changes the time at which the aircraft reaches this altitude, and this time might very well vary from aircraft to aircraft as each aircraft will have its own purposely designed VNRS. Therefore, instead of looking at the limit of 192 seconds for the climb phase, the mass of pollutant emissions is integrated until the time at which the aircraft reaches 3000 ft AGL, as shown in Table 5. The difference between the Standard and Advanced trajectory approximately doubles for CO and decreases to almost 0% for NO_x.

Table 5. Comparison of NO_x and CO emissions mass for take-off and climb-out regime of the conventional LTO cycle for the Standard and Advanced NASA STCA takeoff trajectory.

Limit	Trajectory	m _{NO_x} [g]	Δ	m _{CO} [g]	Δ
192 seconds	Standard	1644	-11.5 %	41	+29.3 %
	Advanced	1455		53	
3000 ft AGL	Standard	1053	-0.6 %	16	+56.3 %
	Advanced	1046		25	

Publications

N/A

Outreach Efforts

Mr. Laurens Voet presented an information paper titled “Investigation of the effects of VNRS on LTO emissions of engines for supersonic transport aircraft” at the CAEP/12-WG3/5-ESTG meeting on November 3, 2020.

Awards

None

Student Involvement

This Task was conducted primarily by Laurens Voet, a graduate research assistant working under the supervision of Dr. Jayant Sabnis, Dr. Raymond Speth, and Dr. Choon Tan.

Plans for Next Period

- Applying this analysis to a wider range of aircraft designs in terms of number of engines, cruise Mach numbers, and maximum tak-off weight (MTOW).
- Applying this analysis to engines with different emissions characteristics to understand whether the emissions LTO cycle is relevant, even if it may not be precisely representative.

References

J. J. Berton, K. Geiselhart (2019). NASA 55-tonne Supersonic Transport Concept Aeroplane (STCA) release package. NASA GRC/NASA LaRC.